Applied Catalysis B: Environmental 170-171 (2015) 283–292

Contents lists available at ScienceDirect

Applied Catalysis B: Environmental

journal homepage: www.elsevier.com/locate/apcatb

Al_2O_3-based passive NOx adsorbers for low temperature applications

Yaying Ji, Shuli Bai, Mark Crocker*

Center for Applied Energy Research, University of Kentucky, Lexington KY 40511, USA

ARTICLE INFO

Article history:
Received 23 October 2014
Received in revised form 16 January 2015
Accepted 20 January 2015
Available online 24 January 2015

Keywords:
Passive NOx adsorber
Alumina
Lanthanum
Adsorption
Desorption
Low temperature

ABSTRACT

NOx storage on Pt/Al_2O_3 and $Pt/La\text{-}Al_2O_3$ in the temperature range 80–160 °C was investigated by means of microreactor and in situ DRIFTS experiments, to ascertain their suitability for passive NOx adsorber applications. Addition of 1 wt% La to Al_2O_3 resulted in the creation of new NOx storage sites and improved NOx storage efficiency. However, according to TPD measurements, $Pt/La\text{-}Al_2O_3$ exhibited slightly lower NOx desorption efficiency below 250 °C than Pt/Al_2O_3. During repeated NOx adsorption–desorption cycles, almost no benefit of La addition was observed after five cycles, due to the inability to regenerate the strong NOx storage sites associated with the La at 250 °C. DRIFTS measurements indicated that during NOx-TPD, nitrites and weakly bound nitrate species were initially removed from the surface of Pt/Al_2O_3 and $Pt/La\text{-}Al_2O_3$. NOx desorption at higher temperatures (>250 °C) was mainly associated with nitrate decomposition. DRIFTS measurements on Pt/Al_2O_3 revealed that NOx was mainly stored on the Al_2O_3 surface when oxidized Pt was present, although when a reductive re-treatment was applied NOx storage on reduced Pt sites became significant and total NOx storage efficiency was improved. However, compared to bare Al_2O_3, NOx desorption efficiency below 250 °C significantly dropped when Pt was present, and was even lower after pre-reduction in H_2. Overall, the Pt-Al without pre-reduction showed the highest amount of NOx desorption below 250 °C.

1. Introduction

The control of NOx emissions from lean-burn engines represents an on-going challenge to the automotive industry, particularly at the low exhaust temperatures associated with modern, fuel-efficient engines. While the factors limiting low temperature NOx control by catalyst-based aftertreatment systems are well recognized, the performance of current catalyst formulations is insufficient at the low exhaust temperatures expected for the new engines under development. For instance, the slow rate of urea decomposition limits the ability to deploy urea-based selective catalytic reduction ("urea SCR") for NOx reduction at low operating temperatures (<180 °C). Consequently, a system is required which combines low temperature NOx storage with subsequent NOx reduction. An attractive option which to date has been little explored is the use of a passive NOx adsorber (PNA) device in combination with a urea SCR catalyst. In this system, the PNA adsorbs NOx emitted from the engine during cold starts, and then releases the NOx at higher temperatures, e.g., above 200 °C. At this point the SCR catalyst is sufficiently warm to function efficiently. This differs from the LNT-SCR concept, in which the LNT catalyst functions as the primary NOx storage/reduction device, the role of the SCR catalyst being to convert NOx slip (emitted mainly in the lean storage phase) with NH_3 which is emitted by the LNT during rich phase regenerations (and which can be stored on the SCR catalyst) [1]. Given that LNT catalysts function poorly below ca. 200 °C, in general they are unsuitable for the abatement of cold start NOx emissions.

Cole [2] reported the application of a passive NOx adsorber to trap cold-start NOx as early as 1997, the NOx adsorber being used in combination with three-way catalysts. The first reference to such a concept for low-temperature lean exhaust aftertreatment appears to be a U.S. patent granted to Ford in 2001 [3]. γ-Al_2O_3 was claimed as the NOx adsorber, promoted with a platinum group metal. In a separate study, Ford workers reported the use of an Al_2O_3-based lean NOx trap (LNT) catalyst for low temperature applications, the high surface area alumina used exhibiting good NOx storage performance at relatively low temperature (250 °C) [4]. A recent patent application by GM [5] claims a PNA system incorporating an external fuel injection system and air pump. If the vehicle shuts down without the PNA having reached its required regeneration (i.e., thermal desorption) temperature, then air and fuel are injected so as to raise the temperature of the PNA until NOx desorption occurs; the desorbed NOx is reduced to N_2 by residual NH_3 stored on the downstream SCR catalyst. In a recent presentation [6], researchers from Cummins presented data which showed that a PNA/urea SCR

* Corresponding author. Tel.: +1 859 257 0295; fax: +1 859 257 0302.
E-mail address: mark.crocker@uky.edu (M. Crocker).

http://dx.doi.org/10.1016/j.apcatb.2015.01.025
0926-3373/

system was able to achieve lower emissions on a light duty (V8) truck than the corresponding urea SCR-only system. A conclusion from this study was that better PNAs are required, particularly with respect to increase of the NOx release temperature (which should not commence below 175 °C) and increased low temperature NOx adsorption capacity (>90% storage efficiency required up to 150 °C). A recent patent by Johnson Matthey [7] has also claimed passive NOx adsorber catalyst systems based on Al_2O_3- or CeO_2-supported Pt/Pd, the objective being to store NOx below 200 °C; above this temperature NOx is released and can be reduced by a suitable reductant. The use of these materials mixed with a zeolite has also been studied [8,9] as a means to abate both NOx and hydrocarbon emissions during cold starts. Besides precious metal-based NOx adsorbers, silver-based NOx adsorber systems have drawn attention in both industry and academia. Indeed, the use of Al_2O_3-supported silver for this purpose has been disclosed in a US patent by GM [10]. Moreover, Olsson and co-workers [11] reported significant NOx storage capacity achieved over an Ag/Al_2O_3 NOx adsorber system at 200 °C.

Al_2O_3, and especially γ-Al_2O_3, has been used in a large number of chemical processes as variously an adsorbent, a catalyst and/or a catalyst support. Given its relatively high specific surface area and its thermal stability, γ-Al_2O_3 (which is often promoted with La_2O_3 to further improve its thermal stability with respect to sintering), has become an important support material in automotive catalysts. Moreover, as indicated above, the sorbent properties of Al_2O_3 render it a promising candidate for low temperature PNA applications. However, NOx storage on Al_2O_3 at low temperatures (<200 °C) has not been widely investigated. For this reason, we have studied NOx storage on Pt/Al_2O_3 and Pt/La-Al_2O_3 using microreactor and in situ DRIFTS measurements in an effort to gain detailed information about the NOx storage and desorption properties of Al_2O_3.

2. Experimental

2.1. Catalyst preparation

Two different kinds of model catalysts were used in this study, namely, Pt/γ-Al_2O_3 and Pt/La-promoted Al_2O_3. Both catalysts were prepared by means of incipient wetness impregnation. γ-Al_2O_3 (Sasol, BET surface area of 201 m^2/g) was impregnated with an aqueous solution of tetraamine platinum (II) nitrate to give a Pt loading of 1 wt%, then dried and calcined at 500 °C for 3 h. The resulting sample is hereafter denoted as Pt-Al. Pt/La-promoted Al_2O_3 was prepared in a sequential manner. γ-Al_2O_3 was first impregnated with an aqueous solution of lanthanum nitrate hexahydrate, then dried and calcined at 500 °C for 3 h. The La-promoted Al_2O_3 was subsequently impregnated with aqueous tetraamineplatinum(II) nitrate and further calcined at 500 °C for 3 h. Samples were prepared with La contents of 1 wt%, 3 wt% and 10 wt%, the Pt loading being fixed at 1 wt% in all cases. The resulting samples are denoted as Pt-1La (Pt/1 wt% La-Al_2O_3), Pt-3La (Pt/3 wt% La-Al_2O_3) and Pt-10La (Pt/10 wt% La-Al_2O_3).

2.2. Catalyst characterization

BET surface area and pore volume measurements were performed by nitrogen adsorption at −196 °C using a Micromeritics Tri-Star 3000 system. Catalyst samples were outgassed overnight at 160 °C under vacuum prior to the measurements. Pt dispersion was determined by means of pulsed H_2 chemisorption at dry ice temperature (−78 °C) using a Micromeritics AutoChem II Analyzer. Around 200 mg of the catalyst was loaded into the reactor. After being reduced at 300 °C in 10% H_2/Ar for 30 min, the catalyst was heated up to 400 °C (hold time 10 min) in flowing Ar to remove adsorbed H. Pulsed H_2 chemisorption was initiated using a four-way valve after the catalyst had been cooled to −78 °C. During this measurement, 0.5 ml of 10% H_2/Ar was pulsed into the reactor every 2 min, the H_2 signal at the reactor outlet being monitored with a thermal conductivity detector (TCD). H_2 pulsing was terminated after the TCD signal had reached a constant value, i.e., the precious metal sites were saturated with H_2. Assuming a 1:1 ratio of atomic hydrogen to surface Pt, the metal dispersion was calculated based on the amount of H adsorbed.

X-ray powder diffraction was conducted on a Phillips X'Pert diffractometer using Cu-Kα radiation (λ = 1.540598 Å). Diffractograms were recorded between 5° and 90° (2Θ) with a step of 0.02°.

X-ray photoelectron spectroscopy (XPS) measurements were performed on a Thermo Scientific K-ALPHA spectrometer using Al-Kα radiation (1486.6 eV) as the X-ray source. The beam was monochromatized by a twin crystal monochromator, yielding a focused X-ray spot with a size of 400 μm^2, at 3 mA × 12 kV. The alpha hemi-spherical analyzer was operated in the constant energy mode with a pass energy of 50 eV. Charge compensation was achieved with a low energy electron flood gun and low energy argon ions from a single source.

2.3. NOx storage efficiency (NSE) and temperature-programmed desorption

A microreactor loaded with ca. 150 mg of powder catalyst was employed to study the NOx adsorption and desorption properties of the catalysts. In all the cases, a total flow rate of 120 sccm was used, corresponding to a gas hourly space velocity (GHSV) of ca. 30,000 h^{-1}. Effluent gases were analyzed using a mass spectrometer (QMS 200). Unless otherwise stated, the catalysts were first pretreated at the desired NOx storage temperature under lean gas containing 5% O_2, 5% CO_2, 3.5% H_2O and He as the balance until the samples were saturated (based on a comparison of the feed and effluent gas concentrations); typically this required 15 min. NOx storage was performed at three different temperatures (80, 100 and 120 °C) by adding 300 ppm NO to the lean feed gas. After NOx storage for a specified period of time, the feed gas was switched to bypass mode and the NO flow was switched off. When the NO concentration had dropped to zero, the gas was re-directed to the reactor and temperature-programmed desorption was carried out to study NOx desorption behavior using a ramp rate of 10 °C/min from the storage temperature up to 500 °C. In one case (Pt-Al), a reductive pretreatment was applied to the sample before NOx storage and desorption. The sample was reduced at 450 °C for 30 min under flowing 1% H_2/Ar (120 sccm), after which the gas flow was switched to flowing Ar (120 sccm) and the temperature was raised to 500 °C and held for 30 min. After that, the catalyst was cooled down to 120 °C in flowing Ar for the NOx storage measurement. In another set of experiments, the Pt-Al and Pt-1La samples were pretreated at 500 °C in 10% O_2/He flow (120 sccm) for 30 min before cooling to 120 °C in flowing Ar. NOx adsorption was then performed for 30 min using a feed gas containing 300 ppm NO, 5% O_2, and He as balance, i.e., in the absence of H_2O and CO_2. NOx desorption was subsequently performed using 5% O_2 in He as the feed gas.

To understand the effect of multiple storage-desorption cycles, cycling experiments were also performed: first, the catalyst was exposed to NOx storage conditions at 120 °C for 10 min, after which TPD was performed up to 250 °C using a ramp rate of 10 °C/min and the same lean feed gas but without the inclusion of NO. Subsequently, the temperature was lowered to 120 °C for the next NOx adsorption–desorption cycle. In total, five cycles were investigated for both Pt-Al and Pt-1La. In these experiments, H_2O and CO_2 were included in the feed gas.

Table 1
Physical properties of the catalysts.

Catalyst	BET SA (m^2/g)	Pore volume (cm^3/g)	Mean pore radius (nm)	Pt dispersion (%)	La/Al atomic ratio (XPS)
Pt-Al	195.5	0.491	5.022	87.0	–
Pt-1La	191.5	0.483	5.049	53.0	0.004
Pt-3La	186.6	0.467	5.033	49.1	0.025
Pt-10La	167.4	0.421	5.031	42.0	0.036

NOx storage efficiency (hereafter denoted as NSE) is defined as the percentage of NOx fed to the reactor that is stored, while NOx desorption efficiency (hereafter denoted as NDE) is defined as the percentage of stored NOx that is desorbed during TPD, i.e.,:

$$\mathrm{NSE} = (1 - \frac{\int_o^t([\mathrm{NOx}]\mathrm{out})\mathrm{dt}}{\int_o^t([\mathrm{NO}]\mathrm{in})\mathrm{dt}}) \times 100\%$$

$$\mathrm{NDE} = (\frac{\int_{t(\mathrm{To})}^{t(\mathrm{T})}([\mathrm{NOx}]\mathrm{out})\mathrm{dt}}{\mathrm{NSE} \times t \times [\mathrm{NO}]\mathrm{in}}) \times 100\%$$

in which t is the NOx storage time; $[NO]_{in}$ is the inlet NO concentration during NOx storage; $[NOx]_{out}$ is the outlet NOx concentration including NO and NO_2 during either NOx storage or the subsequent NOx desorption period; t(To) is the start time of NOx-TPD corresponding to the NOx storage temperature before the temperature is raised; t(T) is the end time of NOx-TPD corresponding to the desired NOx desorption temperature.

2.4. Diffuse reflectance infrared fourier transform spectroscopy

DRIFTS measurements were performed to monitor the surface species involved in NOx adsorption and desorption. Measurements were performed using a Nicolet 6700 IR spectrometer equipped with a Harrick Praying Mantis accessory and MCT detector. The reaction cell was sealed with a dome equipped with two ZnSe windows and one SiO_2 observation window. The temperature of the reactor cell was controlled and monitored by a *K*-type thermocouple placed beneath the reaction chamber. For each DRIFT spectrum an average of 115 scans was collected (requiring ca. 1 min) with a resolution of 4 cm^{-1}. The spectrometer, as well as the outside of the reaction cell, were continuously purged with dry nitrogen to avoid diffusion of air into the system. Unless otherwise stated, catalyst samples (~50 mg) were pretreated in situ in flowing 5% O_2/Ar (120 sccm) at 500 °C for 1 h in order to remove moisture and carbonate, after which background spectra were collected (using the same feed gas) in the range 500–100 °C at intervals of 50 °C. NOx storage was carried out at 100 °C for 30 min using a feed consisting of 5% O_2 and 300 ppm NO (120 sccm). During NOx storage spectra were collected as a function of time. After 30 min of NOx storage, temperature programmed desorption (TPD) was performed in flowing 5% O_2/Ar flow (120 sccm), the temperature being raised from 100 °C to 500 °C at a rate of 10 °C/min. DRIFT spectra were recorded during TPD at intervals of 50 °C. Absorbance spectra were obtained by subtracting background spectra from the spectra collected during NOx storage and desorption.

In one case (Pt-Al), the sample was subjected to a reductive treatment prior to DRIFTS measurements. In this case, the sample was exposed to 1% H_2/Ar at 450 °C for 1 h (ca. 100 sccm), after which the feed gas was switched to Ar and the temperature raised to 500 °C for removal of adsorbed H atoms. All the subsequent background spectra (500 → 100 °C) were likewise collected in Ar (to prevent oxidation of the sample). NOx storage was subsequently carried out at 100 °C as described above.

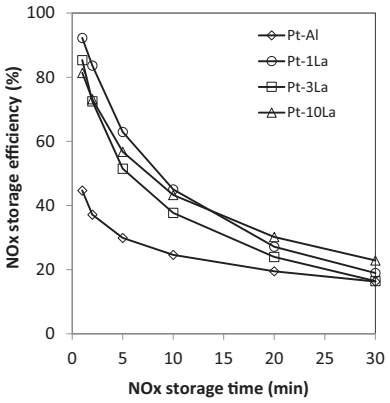

Fig. 1. Comparison of NOx storage efficiency during NOx adsorption at 120 °C. Feed: 300 ppm NO, 5% O_2, 5% CO_2, 3.5% H_2O, He as balance.

3. Results

3.1. Catalyst characterization

To increase the basicity of the γ-Al_2O_3 used in this study, La was added in the concentration range 1–10 wt%. Characterization data for the resulting four catalysts are collected in Table 1. According to N_2 physisorption data, the specific surface areas of the samples decreased with increasing La loading, a 14% decrease being observed when the La loading increased from 0 to 10 wt%. A corresponding drop in pore volume was also observed after introduction of La, the pore volume decreasing from 0.49 cm^3/g for Pt-Al to 0.42 cm^3/g for Pt-10La.

According to H_2 chemisorption results, Pt was highly dispersed on the unmodified Al_2O_3 support. However, on the 1 wt% La-Al_2O_3 support the dispersion was much lower (53.0% versus 87.0%), while increase of the La loading caused a further small decrease in the Pt dispersion (Table 1). XRD analysis revealed that the La-modified samples contained nanocrystalline La_2O_3 at a loading of only 3 wt% (data not shown) – well below the supposed La_2O_3 monolayer value on the Al_2O_3 support – albeit the diffraction peak was very small. While XPS analysis indicated a significant increase in the surface La/Al atomic ratio when the La loading was increased from 1 to 3 wt% (namely, from 0.004 to 0.025), the La/Al atomic ratio increased only modestly (to 0.036) when the La loading was increased to 10 wt%. Together, these results suggest that crystalline La_2O_3 starts to form on the Al_2O_3 surface at relatively low loadings (ca. 3 wt%) and is rather poorly dispersed at the 10 wt% loading.

3.2. Effect of La addition

Fig. 1 compares NOx storage efficiency (NSE) as a function of NOx storage time for the samples at 120 °C. All of the samples showed their highest NSE during the initial stages, NSE decreasing significantly with time. La-promoted Al_2O_3 outperformed the unpromoted analog (Pt-Al), as evidenced by the fact that NSE values for the La-promoted samples were almost double that of Pt-Al after 5 min of NOx storage. However, with increased NOx storage time, the promoting effect of La became less significant, the NSE of

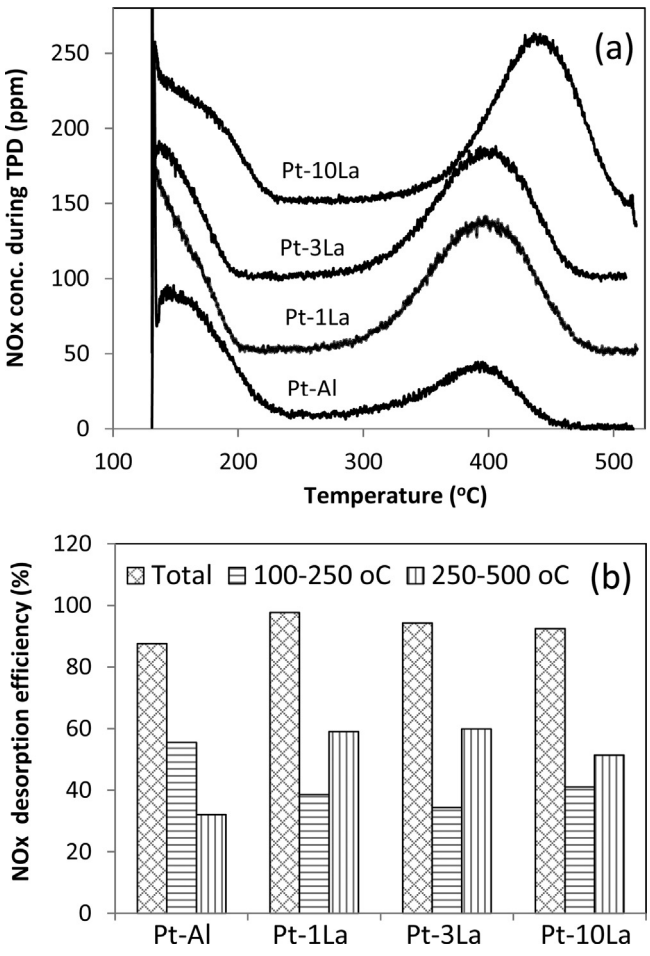

Fig. 2. (a) NOx thermal release profiles during temperature-programmed desorption. Feed: 5% CO_2, 3.5% H_2O, 5% O_2, He as balance. NOx pre-adsorbed at 120 °C for 30 min. (b) Comparison of NOx desorption efficiency for two different temperature ranges (100–250 °C and 250–500 °C).

the promoted samples showing only a marginal advantage at the end of the 30 min storage period compared to Pt-Al.

The results of subsequent NOx-TPD are compared in Fig. 2. As shown in Fig. 2a, in general two NOx desorption events were observed during TPD, the first one occurring below 250 °C (low-temperature NOx desorption) and the second one between 250 and 500 °C (high-temperature NOx desorption). For La loadings between 0 and 3%, the second desorption maximum occurred around 400 °C. A noticeable increase of ca. 40 °C in the position of the desorption maximum was observed for Pt-10La, implying stronger NOx interaction with storage sites at the high La loading.

NOx desorption efficiency (NDE) is compared in Fig. 2b. For TPD up to 500 °C, total NOx desorption efficiency ranks as follows: Pt-1La > Pt-3La > Pt-10La > Pt-Al. Among these four catalysts, Pt-1La displayed a total NDE of 98%, indicative of nearly complete NOx desorption. In contrast, the value for Pt-Al was 88%, indicating that ~12% of the stored NOx remained on Pt-Al even when the temperature was raised to 500 °C. A further comparison was made on the basis of the two individual NOx desorption events (i.e., below 250 °C and between 250 and 500 °C). As seen in Fig. 2b, the NOx desorption efficiency below 250 °C follows the order Pt-Al > Pt-10La ~ Pt-1La > Pt-3La. Ca. 55% of NOx stored on Pt-Al was desorbed below 250 °C, while the La-promoted catalysts achieved values of ca. 40%, indicating that ~60% of the NOx stored at 120 °C required a temperature greater than 250 °C for thermal desorption. Similar to NOx storage behavior, increasing the La loading failed to significantly impact NOx desorption behavior. Therefore, Pt-Al and Pt-1La were chosen for further study.

3.3. Effect of NOx storage temperature

Three different NOx storage temperatures were investigated in this study: 80, 120 and 160 °C. The selection of 80 °C as the minimum storage temperature was based on published data from Ford Motor Co. [12]; specifically, it was shown that the exhaust gas temperature behind the diesel oxidation catalyst of a 4.4 L diesel engine (upstream of the SCR catalyst) reached a value of ~60 °C after about 10 s of the cold start. Consequently, there is little value in studying NOx storage at very low temperatures (e.g., 20 °C). The effect of NOx storage temperature on NSE for Pt-Al and Pt-1La is shown in Fig. 3. For Pt-Al, NSE increased with storage temperature. For example, the 1 min NOx storage efficiency increased by 30% when the temperature was raised from 80 to 160 °C. However, at 160 °C the NSE decreased with storage time more sharply relative to storage at 80 and 120 °C, such that after 30 min of storage there was little difference between the NSE values for the three temperatures. In the case of Pt-1La, increasing the storage temperature from 80 to 120 °C likewise improved the NSE. Increase of the temperature to 160 °C negatively impacted NOx storage capability as shown in Fig. 3b, although at long storage times NSE values were again similar.

The effect of NOx storage temperature on NOx desorption behavior is shown in Fig. 4. As shown in Fig. 4a, the catalysts displayed a common trend, namely, that low temperature NDE (below 250 °C) decreased with increasing NOx storage temperature, implying stronger interaction of NOx with adsorption sites at high NOx storage temperatures. Moreover, Pt-Al showed higher low-temperature NDE than Pt-1La at the three temperatures

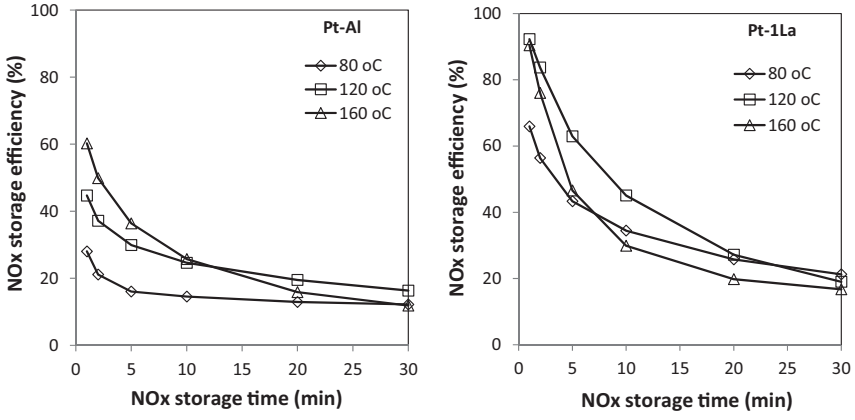

Fig. 3. Effect of temperature on NOx storage efficiency. Feed: 300 ppm NO, 5% O_2, 5% CO_2, 3.5% H_2O, He as balance.

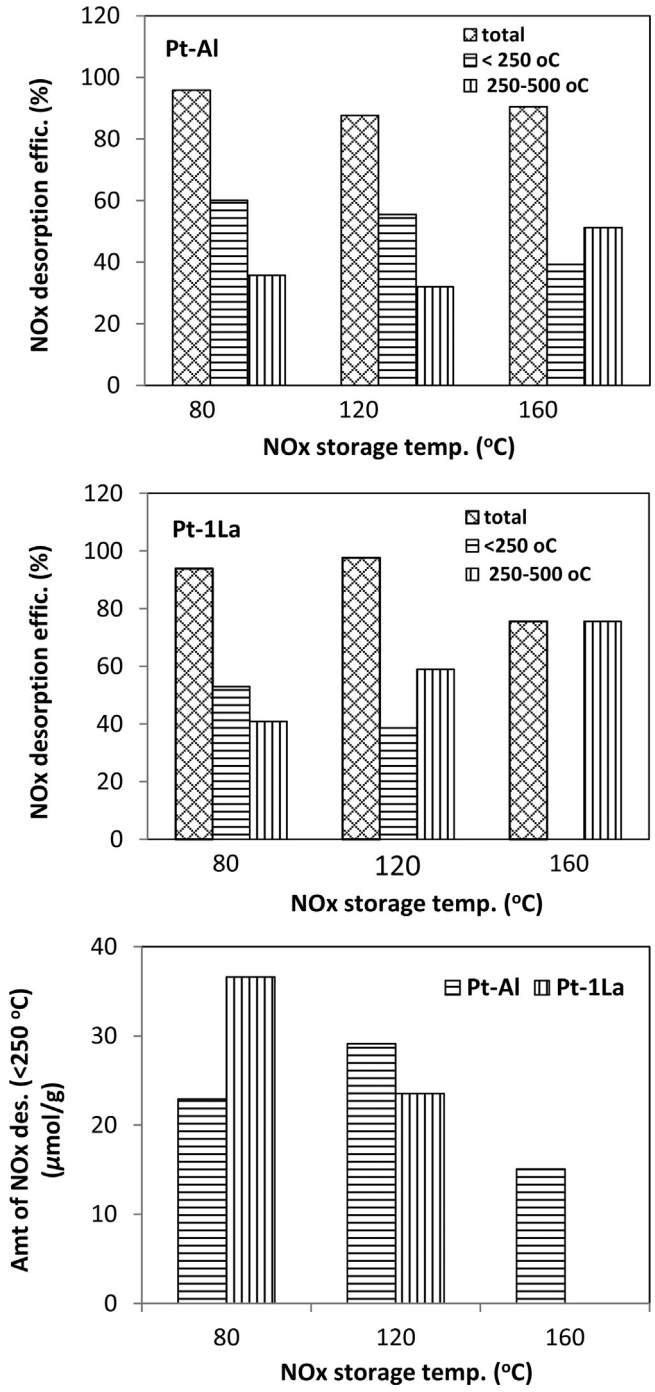

Fig. 4. Effect of NOx storage temperature on NOx desorption efficiency and amount of NOx desorbed below 250 °C (storage time = 30 min).

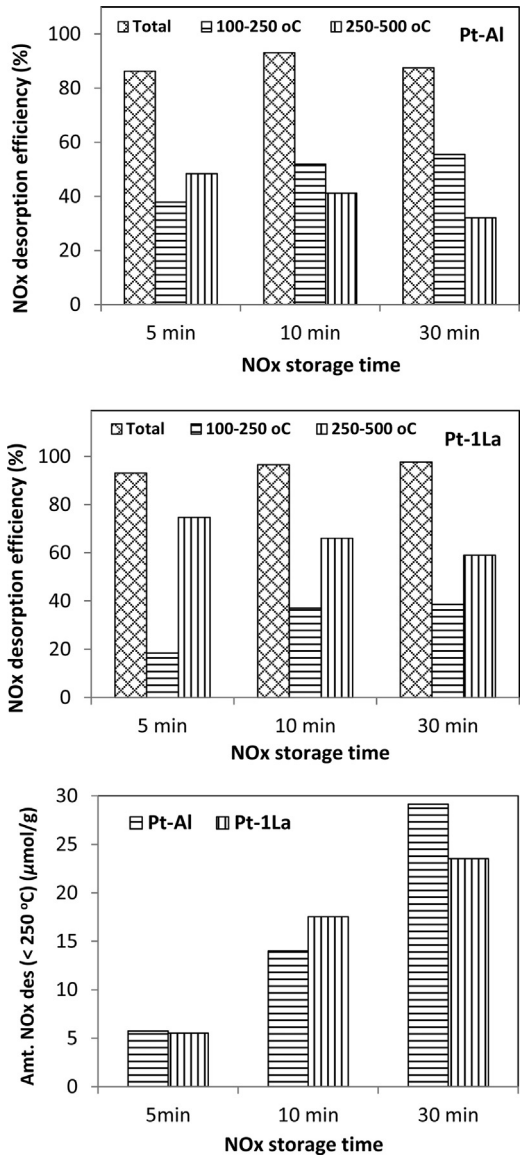

Fig. 5. Effect of NOx storage time on NOx desorption efficiency and amount of NOx desorbed below 250 °C (NOx stored at 120 °C).

investigated. It can be concluded that increasing the NOx storage temperature exerts a positive effect on NOx storage efficiency but a negative effect on NOx desorption efficiency. The combined impact of these two effects is reflected in the amount of NOx desorbed below 250 °C (Fig. 4c). Pt-1La displayed the highest amount of NOx desorbed below 250 °C, corresponding to a storage temperature of 80 °C (36.6 μmol NOx/g_{cat}), while Pt-Al exhibited its highest value after NOx storage at 120 °C (29.1 μmol NOx/g_{cat}). Overall, Pt-1La exhibited better low temperature desorption capability than Pt-Al after NOx storage at 80 °C, whereas after storage at 160 °C the situation was reversed, Pt-1La failing to show any NOx release below 250 °C. After storage at 120 °C, the two catalysts showed similar low temperature NOx release.

3.4. Effect of NOx storage time

The effect of NOx storage time on NOx-TPD was investigated using a NOx storage temperature of 120 °C. Three different storage times were employed: 5 min, 10 min and 30 min. NOx desorption behavior for the different storage times is compared in Fig. 5, from which several trends emerge. First, Pt-1La shows slightly higher total NDE than Pt-Al in all the three cases, while Pt-Al possesses higher low-temperature NDE than Pt-1La. Moreover, low-temperature NDE increased with storage time for both catalysts, implying that at longer storage times NOx is stored on weaker adsorption sites. The total amount of NOx desorbed below 250 °C is compared in Fig. 5. For both Pt-Al and Pt-1La, the total amount of NOx desorbed below 250 °C increased with storage time, and significant increase was observed in the first 10 min for both catalysts, again implying that at longer storage times NOx is increasingly stored on weak sites. As shown in Fig. 5c, comparison of the two catalysts indicates that the benefit of La addition mainly occurs at

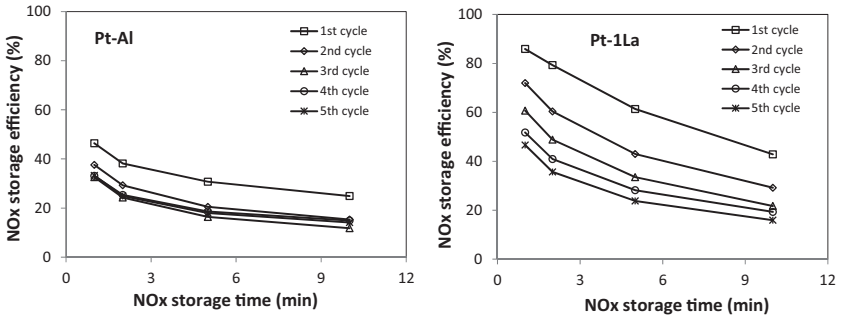

Fig. 6. Comparison of NOx adsorption efficiency during NOx storage at 120 °C (10 min) for consecutive NOx adsorption–desorption cycles.

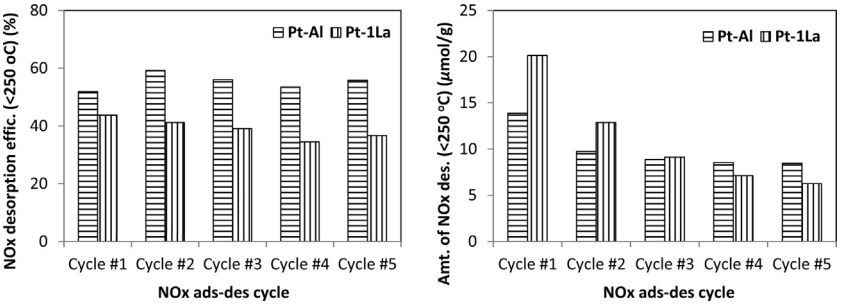

Fig. 7. Comparison of amount of NOx desorbed below 250 °C during TPD for consecutive NOx adsorption–desorption cycles.

short storage times. This can be attributed to the fact that while the low-temperature NDE of Pt-1La is consistently inferior to that of Pt-Al, the NSE of Pt-1La is significantly higher than that of Pt-Al at short to moderate storage times (Fig. 1), resulting in higher overall NOx release. At long NOx storage times (e.g., 30 min) the NSE values of Pt-1La and Pt-Al are similar, and hence the superior low-temperature NDE of Pt-Al causes it to display superior overall low-temperature NOx release.

3.5. Effect of CO_2 and H_2O

Although not of relevance for real world applications, NOx storage and desorption data were collected in the absence of CO_2 and H_2O with the goal of facilitating a more realistic comparison between microreactor data and DRIFTS data (these also being collected in the absence of these components, see Section 3.7). Prior to NOx storage, samples were treated at 500 °C to remove surface carbonates and adsorbed water. As expected, in the absence of CO_2 and H_2O (which can compete with NOx for storage sites), high NSE was obtained for Pt-Al for the first minute, as evidenced by a NSE of 96.8% (relative to 46.7% obtained in the presence of CO_2 and H_2O; see Fig. S1). At the end of 30 min storage, NSE values of 70.9% and 51.9% were achieved for Pt-Al and Pt-1La, respectively (compared to 16.3% and 19.0% under regular conditions). During subsequent NOx-TPD (Fig. S2), two well defined desorption events were observed for both samples, i.e., one in the low temperature range (<250 °C) and one at higher temperature (ca. 250–400 °C). These TPD data are qualitatively similar to those obtained in the presence of CO_2 and H_2O, albeit that in the absence of CO_2 and H_2O the low temperature NOx desorption peak shifted to slightly higher temperature (by ~35 °C) and the high temperature peak shifted to lower temperature (~70 °C). In terms of the NDE, a decrease was found for both samples compared to the measurements with CO_2 and H_2O present (Fig. S3), NDE falling for Pt-Al from 55.5% to 44.5% and for Pt-1La from 38.6% to 10%. Despite this, the amount of NOx desorbed below 250 °C for Pt-Al was almost three times higher in the absence of CO_2 and H_2O, due to the high NSE (see Table S1). In the case of Pt-1La, the low NDE resulted in a slight decrease in the amount of NOx desorbed below 250 °C. This difference in NOx desorption behavior for Pt-Al and Pt-1La can be ascribed to the occupancy of weak NOx adsorption sites by La during catalyst preparation, as discussed below (Section 4).

3.6. Adsorption–desorption cycling study

In a real world application, a PNA would be cycled between ambient temperature (cold start) and an operating temperature at which some degree of NOx desorption would be achieved; for a light duty diesel engine, typical operating temperatures are likely to lie in the range ~180–350 °C. To simulate this, a cycling experiment was performed in which NOx was stored at 120 °C for 10 min (in the presence of CO_2 and H_2O), after which the catalyst was heated to 250 °C to promote thermal release of the stored NOx; in total, this process was repeated five times. Fig. 6 displays the measured NSE for Pt-Al and Pt-1La as a function of cycle number. In the case of Pt-1La, a continuous decrease in NSE was observed for each cycle, the decrease being most marked for the first 3 cycles. After five cycles, Pt-1La failed to reach "steady state" operation, i.e., the NSE failed to reach a constant value. In contrast, no decrease in NSE was observed for Pt-Al after the third adsorption-desorption cycle, i.e., the catalyst reached a stable operating state in which the amount of NOx adsorbed by the catalyst during each cycle reached a constant value.

Turning to the NOx desorption behavior of the catalysts during cycling, as shown in Fig. 7, Pt-Al exhibited consistently higher low-temperature NDE than Pt-1La for each cycle. A slight increase in low-temperature NDE was initially observed over Pt-Al, although after 3 cycles the NDE appeared stable. However, Pt-1La displayed a continuous decrease in NDE during cycling; indeed, the difference in low-temperature NDE between these catalysts increased from 8% (1st cycle) to 19% (5th cycle). The total amount of NOx desorbed below 250 °C during cycling is compared in Fig. 7. For Pt-1La, a large amount of NOx (20 $\mu mol/g_{cat}$) was desorbed below 250 °C during the first cycle, compared to 14 $\mu mol\ NOx/g_{cat}$ for Pt-Al. During sub-

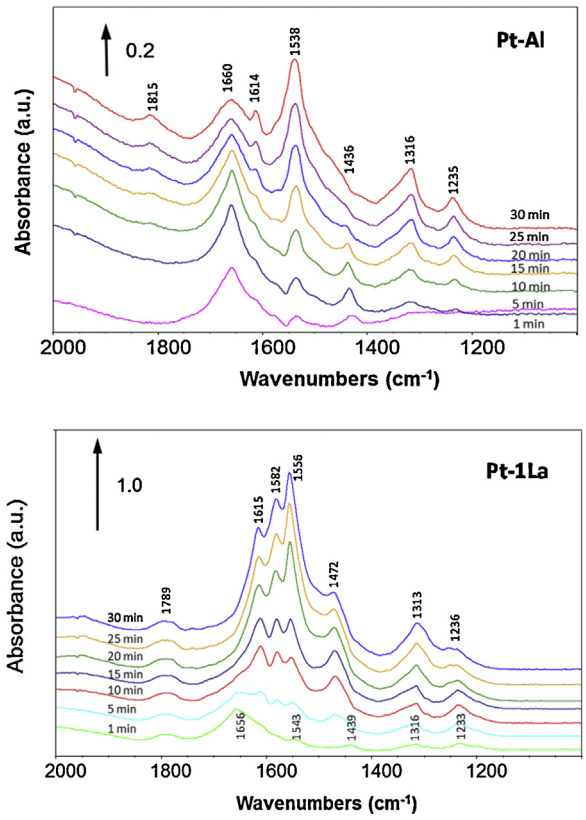

Fig. 8. Evolution of surface species during NOx storage at 100 °C. Feed: 300 ppm NO, 5% O_2, Ar balance. Top: Pt-Al; bottom: Pt-1La.

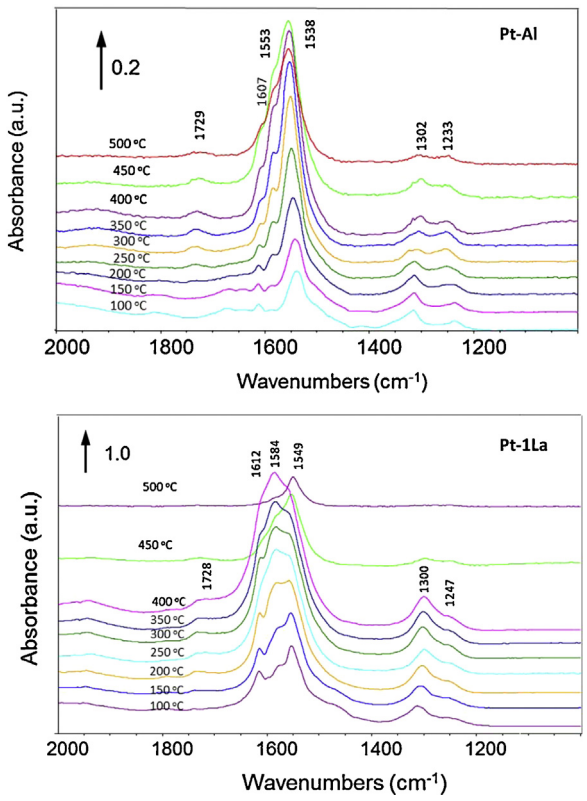

Fig. 9. DRIFT spectra collected during NOx-TPD. Feed: 5%O_2, Ar balance. NOx stored at 100 °C for 30 min. Top: Pt-Al; bottom: Pt-1La.

sequent cycles decreased NOx desorption was observed from both catalysts; however, the extent of this decrease was much smaller for Pt-Al than Pt-1La. By the fourth cycle the amount of NOx desorbed from Pt-Al remained constant, whereas NOx desorption from Pt-1La continued to fall throughout the five cycles, to a value below that of Pt-Al. Notably, neither Pt-Al nor Pt-1La reached a low temperature (below 250 °C) NDE value of 100% during the next cycle.

3.7. *DRIFTS study*

In an effort to gain insight into the mechanism of NOx storage, NOx storage and desorption over Pt-Al and Pt-1La were examined using DRIFTS. Fig. 8 depicts the evolution of DRIFT spectra acquired during NOx storage at 100 °C. For Pt-Al, a band at 1660 cm^{-1} appeared after 1 min, which in the literature has been ascribed to nitrate formed in the vicinity of surface OH groups [13]. TPD experiments described below suggest that this species is very weakly adsorbed (indeed the band almost disappears after NO is removed from the feed), which suggests that it is not a true nitrate species, these generally exhibiting significant thermal stability. For this reason, we tentatively assign this species to NO_2 interacting with OH groups. Simultaneously, two weak bands at 1540 and 1440 cm^{-1} were observed which can be ascribed to nitrate and nitrite species, respectively [14–18]. With increased storage time, almost no growth was observed for the 1660 cm^{-1} band, However, the band at 1540 cm^{-1} continuously grew with time and became the dominant species at the end of the storage period. During this time, the nitrite band appeared to decrease in intensity. In addition, a small shoulder band located at 1610 cm^{-1} became visible at around 10 min. Based on the simultaneous appearance of bands in the range ~1200–1315 cm^{-1}, the bands at 1610 and 1540 cm^{-1} can be ascribed to bridging bidentate and monodentate nitrate, respectively [14–16]. In addition, the formation of bridging bidentate nitrite species cannot be excluded given that they would be expected to give rise to bands at 1320 and 1230 cm^{-1} [15,16], i.e., in the region where bands are indeed observed. Different from the bridging bidentate nitrite, the band at ca. 1440 cm^{-1} is assigned to monodentate (most likely linear) nitrite [17,18]. Finally, a weak band at 1813 cm^{-1} was observed around 15 min, which is most likely related to NO adsorption on Pt (Pt^0/Pt^+—NO) [19,20].

Turning to Pt-1La, similar to Pt-Al, three bands at 1656, 1543 and 1440 cm^{-1} appeared simultaneously at the beginning of NOx storage. Three additional bands located at 1610, 1580 and 1550 cm^{-1} appeared around 5 min and became progressively more intense as the experiment progressed, while related bands grew at 1313 and 1236 cm^{-1}. Based on the literature [14,15], the 1610, 1580 and 1550 cm^{-1} bands can be assigned to bridging bidentate nitrate, chelating bidentate nitrate and monodentate nitrate species, respectively. Of these species, the monodentate nitrates were formed preferentially, being the dominant species toward the end of the NOx storage experiment. Compared to Pt-Al, the absorption bands observed for Pt-1La were significantly more intense, particularly for bridging/chelating nitrate species. These results imply that new NOx storage sites are created when Al_2O_3 is modified by La_2O_3, which explains why Pt-1La shows superior NSE compared to Pt-Al. Another notable observation is the fact that the intensity of the nitrite band remained fairly constant for Pt-1La during the course of the experiment, in contrast to Pt-Al for which the band progressively decreased in intensity after the first 5–10 min.

The evolution of surface species on Pt-Al and Pt-1La during TPD is shown in Fig. 9. After switching to O_2/Ar feed gas at 100 °C, the species at 1660 cm^{-1} ("AlOH–NO_2") on Pt-Al almost immediately disappeared, indicating that NO_2 is weakly adsorbed on the surface OH groups. In contrast, the two nitrate bands (1610 and 1553 cm^{-1}) initially become stronger with increase of the temperature, the monodentate nitrate (1538 cm^{-1}) remaining the

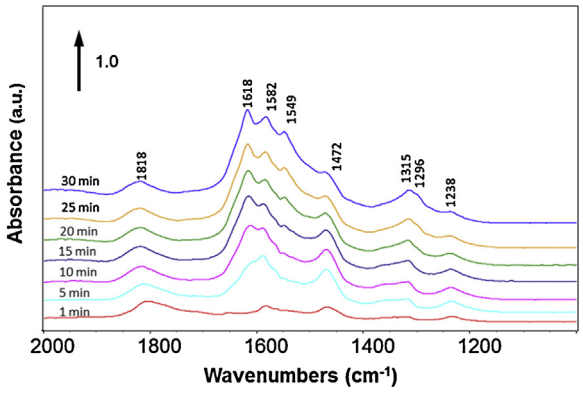

Fig. 10. DRIFT spectra collected for Pt-Al during NOx storage at 100 °C in the absence of O_2.

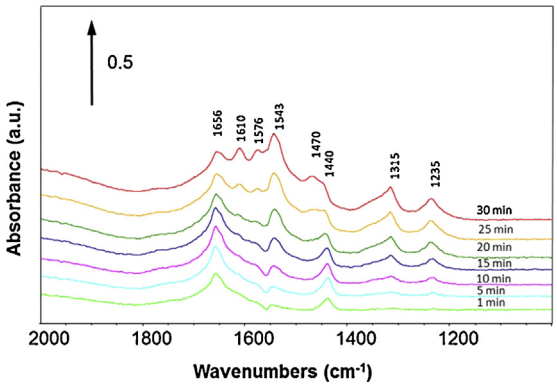

Fig. 11. DRIFT spectra collected for bare Al_2O_3 during NOx storage at 100 °C. Feed: 300 ppm NO, 5% O_2, Ar as balance.

dominant species. This growth of the nitrate species suggests that instead of desorption, one or more NOx species present – such as nitrite- were converted to nitrate species. However, it is noteworthy that as the temperature was raised, subtle changes were observed in the band intensity ratios of the three main nitrate species present (bridging, chelating and monodentate); indeed, as shown in Fig. 9, the nitrate bands at higher wavenumber became more intense relative to the low wavenumber band as the temperature was raised. Therefore, it is not inconceivable that the interconversion of species with very different molar absorption coefficients may be responsible, in part at least, for the initial increase in total nitrate band intensity. Under the oxidizing conditions used, the nitrate species appeared very stable, only undergoing decomposition above 400 °C; this is consistent with results reported by Venkov et al. [13]. A small fraction of the nitrate species still remained on the surface at 500 °C.

In the case of Pt-1La, similar to Pt-Al, OH-bound NO_2 species disappeared at 100 °C when NO was removed from the feed, while nitrite species also appeared to be largely removed. Consequently, bridging bidentate nitrate (1610 cm^{-1}), chelating nitrate (1584 cm^{-1}) and monodentate nitrate (1549 cm^{-1}) became the main surface species present. These nitrate bands grew in intensity with increasing temperature, while their distribution also changed with temperature, the band assigned to chelating nitrate species becoming the most intense signal above 250 °C. A significant drop in the intensity of these three nitrate bands was observed at 450 °C, indicating that most of the nitrate species underwent thermal decomposition at this temperature. At 500 °C, only a small amount of monodentate nitrate species remained on the surface.

3.8. Comparison of NOx adsorption on Al_2O_3, Pt/Al_2O_3 and pre-reduced Pt/Al_2O_3

To provide insights into the mechanism of NOx storage on Al_2O_3-based PNAs, additional DRIFTS and microreactor measurements were performed using Pt-Al and the bare Al_2O_3 support. Fig. 10 depicts DRIFTS spectra collected during NOx storage on Pt-Al in the absence of O_2. Unlike NOx storage in the presence of O_2, a strong band at ca. 1660 cm^{-1} was not observed. This suggests that the 1660 cm^{-1} band is not the product of NO adsorption, i.e., that it is associated with NO_2 adsorption. Instead, intense nitrate (1618, 1582, 1549 cm^{-1}) and nitrite (1472 cm^{-1}) bands appeared. The observation of nitrate bands indicates that even in the absence of O_2 in the feed, surface oxidation of NO can occur. Given that sample pre-treatment occurred in the presence of O_2, it is likely that Pt was present as the oxide, which underwent reduction by NO [21] with subsequent spillover of NO_2 to the alumina and nitrate formation.

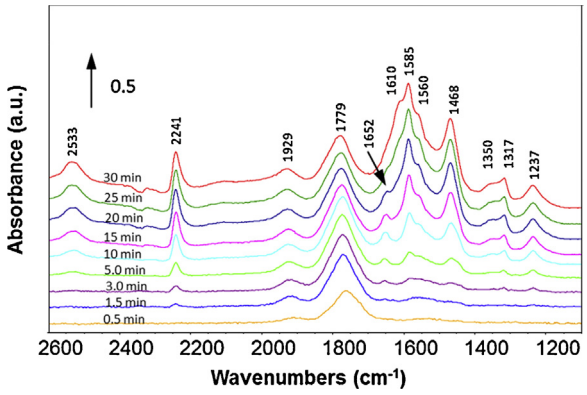

Fig. 12. DRIFT spectra collected for Pt-Al during NOx storage at 100 °C. Feed: 300 ppm NO, 5% O_2, Ar as balance. Note: the catalyst was pretreated with H_2 at 450 °C for 30 min.

A comparison was also made of NOx adsorption on Pt-Al and Al_2O_3 (no Pt added). As shown in Fig. 11, DRIFTS spectra collected over Al_2O_3 during NOx storage at 100 °C in the presence of O_2 showed similar bands to Pt-Al (Fig. 8, top), although the distribution of these bands is not exactly the same as for Pt-Al. However, this implies that NOx is stored mainly on Al_2O_3 rather than Pt. This is consistent with the observation of only a very weak band corresponding to Pt-based NO species (ca. 1813 cm^{-1}), the relative lack of stable, adsorbed NOx species on Pt being ascribed to the oxidized state of the Pt. To explore this point, DRIFTS measurements were performed during NOx storage at 100 °C on Pt-Al which was first reduced under flowing H_2 at 450 °C for 1 h. As shown in Fig. 12, in addition to intense nitrate (1610, 1585, 1560 cm^{-1}) and nitrite (1468, 1350 cm^{-1}) bands, new bands appeared at 1779 cm^{-1}, 1929 cm^{-1}, 2241 cm^{-1} and 2533 cm^{-1}. The broad band at 1779 cm^{-1} is assigned to linear Pt^0-NO species [22,23], this band being the first band to appear at short storage times. Moreover, the intensity of this band implies that NOx storage on Pt can make a significant contribution to the overall NOx storage capacity. The bands at 1929, 2241 and 2533 cm^{-1} are related to three different types of NO adsorption, corresponding to mononitrosyl ($NO–Al^{3+}$), $NO^+–Al^{3+}$ and $NO^-–Al^{3+}$ species, respectively [11,24]. Apparently, the reductive treatment of Pt-Al prior to NOx storage results in increased NOx storage on both Al_2O_3 and Pt sites.

To further confirm the role of Pt in NOx storage and desorption, additional microreactor experiments were performed, comprising NOx adsorption (at 120 °C) and desorption, for bare Al_2O_3 and pre-reduced Pt-Al. As shown in Fig. 13, bare Al_2O_3 showed lower NSE compared to Pt-Al. The NSE value for the first 2 min doubled after the addition of Pt, demonstrating the promotional role of Pt in NOx

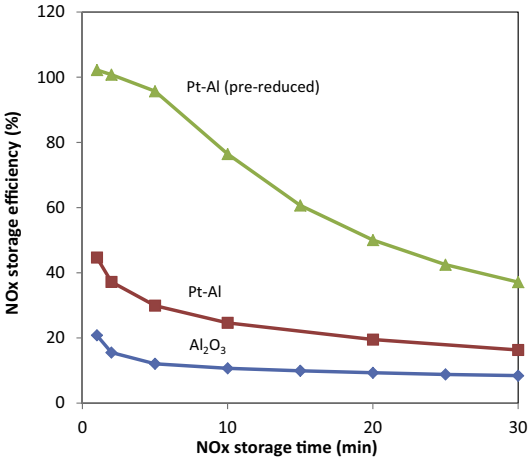

Fig. 13. NOx storage efficiency at 120 °C as a function of storage time for three samples: bare Al_2O_3, Pt-Al, and pre-reduced Pt-Al.

storage. Notably, a pre-reduction treatment (prior to NOx storage) caused tremendous improvement in the NSE, as evidenced by a NSE value of 100% for the first 2 min of NOx storage for pre-reduced Pt-Al. Unfortunately, the reverse effect was observed on NOx desorption behavior, as demonstrated by NDE below 250 °C decreasing in the order: Al_2O_3 > Pt-Al > pre-reduced Pt-Al (see Table 2).

4. Discussion

NOx storage efficiency measurements indicate that the addition of 1 wt% La to Al_2O_3 results in the creation of new NOx storage sites, a fact which can be attributed to the higher basicity of La_2O_3 compared to Al_2O_3. This is reflected in increased NSE at storage times of <30 min. However, further increase in the La loading failed to increase the NSE. Both XRD and XPS analysis confirmed that there was a poor La dispersion on the Al_2O_3 surface at the 10 wt% loading, albeit this is below the supposed monolayer value. The small surface La/Al atomic ratio at the loading of 1 wt% is likely due to the fact that at low loadings La occupies defect sites in the Al_2O_3 structure [25]. Presumably, some of those defect sites were buried in the Al_2O_3 and hence not all of the La was detected by XPS. Indeed, in a recent study Kwak et al. utilized solid-state ^{27}Al NMR to demonstrate the presence of defect sites in the Al_2O_3 surface [26], which were assigned to coordinatively unsaturated pentacoordinate Al^{3+}. At low loadings, Pt preferentially resides on these defect sites, resulting in high dispersions. In this study, the observed decrease in the Pt dispersion (from 87% to 53%) after doping with 1 wt% La may be due to the occupancy of these defect sites by La, forcing Pt to adsorb on sites where it is less strongly bound. The formation of nanocrystalline La_2O_3 at the 3 wt% La loading also demonstrated that the La was no longer highly dispersed on the Al_2O_3 surface after the defect sites were fully occupied. The fact no further improvement in NSE was achieved at the La loadings above 1 wt% suggests that the poor dispersion of the La phase limited its ability to adsorb NOx effectively. Alternatively, it can be speculated that, as if seems likely, the Pt particles are located primarily on the Al_2O_3 surface rather than on the crystalline La_2O_3 phase, inefficient NOx spillover from the Pt particles to the La_2O_3 phase limited NOx adsorption on this phase.

According to TPD measurements, Pt-1La generally exhibits slightly lower NDE below 250 °C than Pt-Al. However, due to the fact that Pt-1La was able to store more NOx than Pt-Al, the amount of NOx desorbed below 250 °C by Pt-1La was in some cases greater, in absolute terms, than for Pt-Al. This was mainly the case for NOx stored at low temperatures (80–120 °C) for relatively short periods. However, the results of adsorption–desorption cycling experiments revealed almost no benefit of La addition with respect to NOx storage or desorption after the third cycle. Although the formation of strong NOx adsorption sites by doping with La significantly improves the initial NOx storage efficiency, these strong sites cannot usefully participate during cyclic operation, i.e., they cannot be regenerated at 250 °C. On the contrary, their creation appears to result in the loss of weak NOx storage sites which are located on Al_2O_3, as demonstrated by the lower amount of NOx desorbed from Pt-1La, compared to Pt-Al, after three or more adsorption-desorption cycles. To develop more efficient Al_2O_3-based PNA materials, it is evident that new sites must be introduced which can function as relatively weak NOx adsorption sites.

Notably, during adsorption–desorption cycling neither Pt-Al nor Pt-1La reached 100% NDE (below 250 °C) during the next cycle. This is significant, given that after several adsorption-desorption cycles, NOx should be mainly adsorbed on weak adsorption sites (the strong adsorption sites having been mostly filled); despite this, it is evident that a portion of the adsorbed NOx cannot be desorbed below 250 °C. A possible reason for this is provided by the DRIFTS measurements discussed below, from which it is evident that a portion of the weakly adsorbed NOx species such as nitrite and OH-bound NO_2 can be converted to (more thermally stable) nitrate species during heating to 250 °C, instead of undergoing thermal release during desorption. Another possible reason why the NDE does not reach 100% is that NOx initially adsorbed on weak sites may migrate to strong adsorption sites. The latter may correspond to subsurface sites or sites that residue far from Pt (assuming that NOx adsorption initially occurs mainly at Pt with subsequent spillover to the alumina), i.e., sites that are kinetically inaccessible during the 10 min adsorption phase, but which are accessible during the subsequent temperature ramp. Either way, these results imply that upon prolonged adsorption-desorption cycling, a new equilibrium would eventually be established, corresponding to saturation of all but the weakest/most kinetically accessible storage sites.

As indicated above (Section 3.7) DRIFTS data imply that NOx thermally released below 250 °C, corresponding to the first desorption event observed during microreactor NOx-TPD studies, arises mainly from desorption of one or more NOx species such as OH-bound NO_2 and/or nitrite species. At higher temperatures (~400–500 °C), thermal decomposition of nitrate species represents the main source of released NOx. However, the fact that nitrate bands initially grow in intensity during TPD implies that some of the nitrite and/or OH-bound NO_2 species can be converted to nitrate species instead of undergoing thermal release. Nitrate species are very stable under oxidizing condition, some of them remaining on the surface at temperatures up to and including 500 °C.

Notably, the reductive treatment of Pt-Al prior to NOx storage results in significantly increased NSE, DRIFTS data being consistent with increased NOx storage on both Al_2O_3 and Pt sites. This improved NOx storage on Al_2O_3 can be explained by several factors. First, metallic Pt is more active for NO oxidation as opposed to oxidized Pt as reported in the literature [21,27]. This is because the binding ability of Pt oxide toward O, O_2 and NO is weaker than metallic Pt. Indeed, the activation energies for NO oxidation are different over oxidized Pt compared to metallic Pt [28]. Therefore, increased NO_2 formation can be expected over reduced Pt during NO storage, leading to increased nitrate formation on the alumina. Second, NO spillover from Pt to Al_2O_3 should be improved due to increased NO adsorption on metallic Pt sites. Indeed, Al_2O_3-based NO bands ($NO—Al^{3+}$, $NO^+—Al^{3+}$ and $NO^-—Al^{3+}$) were observed during NOx storage on the pre-reduced sample.

Finally, it is noteworthy that the addition of Pt significantly weakened low-temperature NOx desorption efficiency, while a

Table 2
Comparison of NDE and amount of NOx desorbed up to 250 °C.

	NDE, <250 °C (%)	Amount of NOx desorbed, <250 °C (μmol/g_{cat})
Al_2O_3	88.3	25.9
Pt-Al	55.5	29.1
Pt-Al (pre-reduced)	9.2	11.0

more significant drop in NDE took place after the pre-reduction treatment, such that less than 10% of stored NOx was thermally released below 250 °C. The amounts of NOx desorbed below 250 °C are compared in Table 2. The Pt-Al sample displayed the highest overall amount of NOx desorbed, the pre-reduced Pt-Al sample displaying the worst overall NOx desorption efficiency (and lowest amount of NOx desorbed). From this it follows that both pretreatment and storage conditions significantly impact NOx storage and desorption behavior over Pt-promoted Al_2O_3-based PNA materials. Specifically, it is apparent that a strongly oxidizing Pt function, while beneficial for NOx storage, inhibits low temperature NOx release during TPD under oxidizing conditions. This can be attributed to the ability of metallic Pt to oxidize released NO to NO_2, which can then be readsorbed to form thermally stable nitrates. In the case of oxidized Pt, a better balance is achieved between NOx storage and desorption, due to the weaker oxidizing function of the Pt. When Pt is absent, as for the bare alumina, the other extreme is reached: NSE is poor, whereas NOx desorption efficiency is high, resulting in the release of moderate amounts of NOx at low temperatures.

5. Conclusions

The NOx storage and desorption properties of Al_2O_3-based PNA materials were investigated using microreactor and DRIFTS measurements. Addition of La enhanced NOx storage efficiency during short NOx storage periods but resulted in a deterioration in NOx desorption efficiency below 250 °C (irrespective of whether CO_2 and H_2O were present or not). DRIFTS results confirmed that higher concentrations of nitrate species formed on the La-promoted sample relative to Pt/Al_2O_3. During NOx adsorption-desorption cycling, repeated cycles resulted in a significant decrease in the NOx storage capacity, accompanied by a continuous decrease in low-temperature NOx desorption efficiency (<250 °C). These effects were more significant for the La-promoted Pt/Al_2O_3 sample, with the consequence that it desorbed smaller amounts of NOx below 250 °C after five cycles than the Pt/Al_2O_3 analog.

DRIFTS measurements indicated that during NOx-TPD, nitrites and other weakly bound species were initially removed from the surface. Additionally, some of the weakly bound NOx species present were converted to strongly adsorbed nitrate species, the nitrates being thermally stable under oxidizing conditions up to 400 °C. The DRIFTS data also implied that NOx was mainly stored on Al_2O_3 when Pt was oxidized, i.e., when the sample was pretreated under lean conditions. However, application of a reduction treatment prior to NOx storage significantly improved the NOx storage efficiency of Pt/Al_2O_3. In this case NOx species adsorbed on the Pt sites were observed, in addition to NOx stored on Al_2O_3. Hence, when metallic Pt is present, the contribution of NOx stored on the Pt sites cannot be ignored with respect to the overall NOx storage capability. The powder reactor study further confirmed the promotional role of Pt in NOx storage and even more significant improvement in NOx storage efficiency after Pt was reduced. However, NOx desorption efficiency was negatively impacted by Pt addition especially after Pt was reduced. Overall, the unreduced Pt-Al showed the best low temperature NOx desorption capability.

Acknowledgements

The authors thank Dr. Dali Qian and Shelley Hopps for XPS and XRD measurements, respectively, as well as Drs. Christine Lambert and Joe Theis of Ford Motor Co. for helpful discussions. Sasol is thanked for a gift of γ-Al_2O_3. This project was funded by the National Science Foundation and theU.S. Department of Energy (DOE) under award no. CBET-1258742. However, any opinions, findings, conclusions, or recommendations expressed herein are those of the authors and do not necessarily reflect the views of the DOE.

Appendix A. Supplementary data

Supplementary data associated with this article can be found, in the online version, at http://dx.doi.org/10.1016/j.apcatb.2015.01.025.

References

[1] J. Wang, Y. Ji, G. Jacobs, S. Jones, D.-J. Kim, M. Crocker, Appl. Catal. B 148–149 (2014) 51.
[2] J. A. Cole, U.S. Patent 5656,244, Energy and Environmental Research Corporation (1997).
[3] M. Jarvis, K.M. Adams, U.S. patent 6182,443, Ford Global Technologies (2001).
[4] L. Xu, G. Graham, R. McCabe, Catal. Lett. 115 (2007) 108.
[5] E.V. Gonze, M.J., Paratore, J.C. Bedford, U.S. patent application 2012/0117947, GM Global Technology Operations (2012).
[6] C. Henry, D. Langenderfer, A. Yezerets, M. Ruth, H.-Y. Chen, H. Hess, M. Naseri, Passive catalytic approach to low temperature NOx emission abatement, in: Presentation at the 2011 DEER Conference, Detroit, MI, 2011.
[7] J.E. Melville, R.J., Brisley, O., Keane, P.R., Phillips, E.H. Mountstevens, U.S. Patent 8105,559, Johnson Matthey Public Limited Company (2012).
[8] H. Chen, S., Mulla, U.S. Patent Pub No. 2012/0308439 A1, Johnson Matthey Public Limited Company.
[9] H. Chen, S. Mulla, E. Weigert, K. Camm, T. Ballinger, J. Cox, P. Blakeman, Technical Paper Series, SAE, 2013, pp. 1–535.
[10] C.K. Koch, G., Qi, S.J., Schmieg, W., Li, U.S. patent pub. No. 2013/0294990 A1, GM Global Technology Operations (2013).
[11] S. Tamm, S. Andonova, L. Olsson, Catal. Lett. 144 (2014) 674.
[12] G. Guo, D. Dobson, J. Warner, W. Ruona, C. Lambert, Technical Paper, Society of Automotive Engineers, 2012, pp. 1–371.
[13] T. Venkov, K. Hadjiivanov, D. Klissurski, Phys. Chem. Chem. Phys. 4 (2002) 2443.
[14] B. Westerberg, E. Fridell, J. Mol. Catal. A 165 (2001) 249.
[15] K. Hadjiivanov, Catal. Rev. -Sci. Eng. 42 (2000) 71.
[16] F.C. Meunier, V. Zuzaniuk, J.P. Breen, M. Olsson, J.R.H. Ross, Catal. Today 59 (2000) 287.
[17] W.S. Kijlstra, D.S. Brands, E.K. Poels, A. Bliek, J. Catal. 171 (1997) 208.
[18] J. Luo, W.S. Epling, G. Qi, W. Li, Catal. Lett. 142 (2012) 946.
[19] F. Prinetto, G. Ghiotti, I. Nova, L. Lietti, E. Tronconi, P. Forzatti, J. Phys. Chem. B 105 (2001) 12732.
[20] F. Boccuzzi, E. Guglielminotti, Surf. Sci. 271 (1992) 149.
[21] K. Hauff, U. Tuttlies, G. Eigenberger, U. Nieken, Appl. Catal. B 123–124 (2012) 107.
[22] P.J. Levy, V. Pitchon, V. Perrichon, M. Primet, M. Chevrier, C. Gauthier, J. Catal. 178 (1998) 363.
[23] A. Bourane, O. Dulaurent, S. Salasc, C. Sarda, C. Bouly, D. Bianchi, J. Catal. 204 (2001) 77.
[24] D.V. Pozdnyakov, V.N. Filimonov, Kinet. Catal. 14 (1973) 665.
[25] B. Beguin, E. Garbowski, M. Primet, Appl. Catal. 75 (1991) 119.
[26] J.-H. Kawk, J. Hu, D. Mei, C.-W. Yi, D.-H. Kim, C.H.F. Peden, L.F. Allard, J. Szanyi, Science 325 (2009) 1670.
[27] W. Hauptmann, Ph.D. Thesis, Technische Universtitat Darmstadt, 2009.
[28] H.-F. Wang, Y.-L. Guo, G. Lu, P. Hu, J. Phys. Chem. C 113 (2009) 18746.